https://doi.org/10.1016/j.jclepro.2017.07.228

Suitability of PoroElastic Road Surface (PERS) for Urban Roads in Cold Regions: Mechanical and Functional Performance Assessment

ABSTRACT

Reuse of scrap tires has become a challenge with the ever-growing traffic volume and usage of vehicles in recent years. Poroelastic Road Surface (PERS) is a novel type of pavement surface, which recycles tire rubber into low-noise pavements. This study aims to explore the suitability of PERS for urban roads in cold regions. Both laboratory tests and numerical simulations were conducted to characterize the mechanical and functional performances of PERS using a conventional porous asphalt (PA) as reference. The results indicated that the tensile strength reserve, which is the difference between the average tensile strength and the cooling-related tensile stress at a certain temperature, of PERS is higher than that of the PA at low temperature, while the ultimate tensile strain of the PERS is much larger than PA. The sound absorption coefficients of PERS have higher and wider peak compared with PA, indicating better noise absorption performance. The pavement with PA surface is more prone to surface cracks due to large tensile stresses at some specific offset locations from the loads, which do not exist in PERS. The deformation of the ice layer on top the PERS layer is larger than that on top of the PA layer at the same temperature, and the maximum horizontal strain of the PERS layer is larger than that of the PA. These findings prove the suitability of PERS for urban roads in cold regions, which can lead to significant economic and social benefits.

Keywords: Poroelastic road surface, cold region, de-icing system, low temperature cracking, acoustic properties

1. INTRODUCTION

With the ever-growing traffic volume and usage of vehicles, the demand on tire production and disposal has significantly increased in recent years. Approximately 5 million tonnes of waste tires were generated every year worldwide, making the reuse of scrap tires a challenge since the rubber, which is the main content of the scrap tires, takes nearly 600 years to decompose completely (Singh et al., 2009, de Almeida Júnior et al., 2012). One of the solutions is to recycle the scrap waste tires into civil engineering materials, such as pavement materials. For example, the ground tire rubber can be added into paving asphalt, which has been found to be an economically and environmentally friendly solution due to the less need for new raw materials and improvement of the performance and service life of asphalt pavements (Siddique and Naik, 2004, Presti, 2013, Shu and Huang, 2014, Estevez, 2009, Yu et al., 2016, Yu et al., 2017, Leng et al., 2017).

Among various applications of waste tyre rubber in pavement, Poroelastic Road Surface (PERS), is relatively recent. PERS is mainly composed of tire rubber granules (most are from scrapped tires), polyurethane, some supplemental materials, such as sand, rocks or other friction-increasing additives, and large air void, (Sandberg et al., 2010, FEHRL, 2006, Amundsen, 2005, Meiarashi, 2003, Sandberg and Kalman, 2005, Sandberg et al., 2005). It is a low-noise road surface material invented as the continuous development of porous asphalt (PA). The noise reduction function of PA pavement mainly relies on its large air void contents (18% to 25%). Compared with PA, PERS has even higher air void contents (up to 40%). In addition, the usage of high amount of rubber particles makes PERS highly elastic and extremely porous, providing even better tire-road noise reduction performance compared with PA (FEHRL, 2006, Sandberg et al., 2010, Amundsen, 2005). To enhance the bonding between rubber and aggregate particles, polyurethane is typically used as the binder in PERS instead of bitumen.

PERS was developed in Sweden in the late 1970's. In the mid 1990's, the Public Works Research Institute (PWRI) in Japan gained interest in the concept and constructed a number of test tracks, which were in service for up to three years. From 2004 to 2008, some PERS test tracks were built in Sweden and the Netherlands, and noise reductions of approximately 8 dB(A) were reported (Amundsen, 2005, FEHRL, 2006, Meiarashi, 2003, Sandberg et al., 2010, Sandberg and Kalman, 2005, Sandberg et al., 2005). In September 2009, a six-year project named PoroElastic Road Surface to Avoid Damage to the Environment (PERSUADE) was launched to develop PERS from an experimental concept to the stage of a practically usable noise abatement measure (Sandberg and Goubert, 2011, Kalman et al., 2011, Pigasse et al., 2012). Various performances of PERS were investigated in this project, including noise reduction capacity, mechanical and aerodynamic noise excitation, and safety, wearing resistance and durability. The existing studies have proved that PERS provided outstanding performance in tire-road noise reduction, which was up to 10-12 dB(A), while the quietest conventional low-noise pavement, double-layer PA, rarely yields reductions exceeding 7 dB(A) (Sandberg and Goubert, 2011, Kalman et al., 2011, Pigasse et al., 2012, Sandberg and Gucbert, 2011, Biligiri et al., 2013). Although PERS provides outstanding performance in noise reduction, it faces the performance concern of low ravelling resistance, which significantly reduces its service life and prevents it from wider application (Goubert et al., 2016, Goubert, 2014, Schacht et al., 2011). In the authors' previous studies (Wang et al., 2017, Schacht et al., 2011), 20 PERS mixtures with different compositions were designed and characterized after various stages of polishing applied by the Aachener-Raveling-Tester (ARTe) (Wang et al., 2015, Wang et al., 2013, Wang et al., 2014). Besides, the high temperature rutting resistance of PERS was also investigated in (Wang et al., 2017, Schacht et al., 2011). It was concluded that binder content and degree of compaction are the critical factors affecting the ravelling resistance of PERS, and a minimum binder content of 15% and a minimum compaction degree of 98% were recommended to ensure sufficient durability. In addition, it was found that there was almost no rutting in PERS samples at the end of the rutting resistance test due to its high elasticity.

Since PERS is a relatively new type of pavement surface, the existing studies have mainly focused on its application in regions with normal weather condition, while its application in cold regions, especially for the urban roads in cold regions, has been seldom investigated. Correspondingly, this study has been conducted to explore the suitability of PERS for urban roads in cold regions.

Compared with conventional roads, the urban roads in cold regions carry the following specific features:

- The urban roads in cold regions are subjected to huge temperature difference between summer and winter. For example, in Harbin, a northeastern city in China, the lowest temperature in winter is about -40°C, while in summer, the temperature can be as high as 40°C.
- Normally, there is large traffic volume on urban roads, but seldom heavy traffic loads. Due to the large traffic volume, loud traffic noise is often a concern for surrounding residents.
- Ice layer may form at the road surface in winter, which significantly reduces the pavement skid resistance. When porous road surfaces, such as PA and PERS, are used, the conventional de-icing methods by using sands and salt have several disadvantages, such as large consumption of the de-icing materials in porous medium and clogging of the pores, in addition to being not environmentally friendly.

Compared with conventional pavement materials, the elastic modulus of PERS is much lower because of the usage of high amount of elastic rubber particles. Therefore, the deformation of PERS is much larger than those of conventional materials subjected to traffic loads. As a result, the interface bonding between the PERS and ice should be easier to be destroyed than that between the conventional pavement materials and ice, and theoretically the ice layer on the PERS is easier to break. If the suitability of PERS for the urban roads in cold regions is proved by this study, PERS can be designed and constructed in cold regions to de-ice in an active manner in addition to providing the function of traffic noise reduction, thus leading to significant economic and social benefits.

To achieve the objective this study, the design of PERS with best ravelling resistance from the previous studies was considered in this study (Wang et al., 2017, Schacht et al., 2011). Its mechanical performance in a wide temperature range and functional performance, such as acoustic properties and de-icing capability, were characterized in laboratory and compared with those of a conventional PA. Besides, finite element method (FEM) was applied to simulate the mechanical responses of pavements surfaced with the PERS and PA with/without ice layer at different temperatures, in order to investigate the mechanical performance of the different pavement surface materials and their de-icing capabilities.

2. EXPERIMENTAL PROGRAM AND RESEARCH METHODOLOGY

2.1 Test samples

Based on the experiences in Sweden, Norway, Japan and the Netherlands, the ravelling resistance of PERS is one of the most important mechanical properties of PERS. Therefore, the effects of following factors on PERS's ravelling resistance were investigated in the authors' previous studies (Wang et al., 2017, Schacht et al., 2011): coarse rubber granule content, fine rubber granule content, quartz sand content, binder content, and degree of compaction (Sandberg et al., 2005, Sandberg and Kalman, 2005, Meiarashi, 2003, Amundsen, 2005, FEHRL, 2006, Sandberg et al., 2010). The ravelling resistance of PERS was evaluated by measuring the granule loss after polishing by the advanced Aachener-Raveling-Tester (ARTe) with real vehicle tires. Based on the test results of ravelling resistance, the PERS mixture exhibiting the best ravelling resistance was identified and selected in this study. The replicates were prepared for further mechanical and acoustic performance analysis in this study.

The air void content of the selected PERS was approximately 35%. The sizes of fine rubber granules and coarse rubber granules were 0.2-0.8mm and 3.1-6.0mm, respectively. The polyurethane product Elastopave® 6551/102 supplied by BASF Polyurethanes GmbH (Lemförder, Germany) was used as the binder. It is a two-component commercial polyurethane binder specially designed for pavement applications. The two components of the binder are polyol mixture (A-component) and diphenylmethane diisocyanate (B-component). **错误!未找到引用源。** shows the pictures of the major components of PERS as well as a compacted PERS sample.

PA with 8 mm nominal maximum aggregate size (PA 0/8), which is commonly used in surface layers for heavy-duty highways in Germany, was selected as a reference material in this study, as both PA and PERS are used as low-noise road surface materials. Its air void content was 26.2 Vol.-% and the binder was polymer modified bitumen (40/100-65 A). The gradation curves of both mixtures are presented in **错误!未找到引用源。**.

2.2 Mechanical Performance: Low-temperature Cracking Resistance

In cold regions, the extremely low temperature can be as low as ca. -30°C. In such case, low-temperature cracking resistance of PERS and PA samples must be considered and measured.

To determine the resistance of the PERS and PA samples to low-temperature cracking, the uniaxial tension stress test (UTST) was performed according to EN 12697-46. The influence of temperature on the behaviour of the samples was measured at four different temperatures: -25°C, -10°C, 5°C and 20°C. The tensile strength and tensile strain at failure were recorded. A higher tensile strength means a higher resistance against cracking and winter damage, while a higher failure tensile strain indicates a longer cracking stage (Teltayev, 2014, Moon et al., 2014, Wen et al., 2015, Arand, 1991). The setup of the device and an illustration of the specimen are given in **错误!未找到引用源。**.

The cooling-related tensile strength was also measured to estimate the low temperature cracking resistance of the specimens. Cooling-related stresses refer to those stresses caused by the temperature change within the specimen. The testing machine is same as that for UTST. The test specimen is fixed on the device and the distance between the two ends remains unchanged. The starting temperature of the experiment is 20°C, and the temperature descending rate is -10K/h. Cooling-related tensile stress is measured and recorded as a function of temperature until the specimen breaks.

A representative example of the test results from UTST and cooling test is given in **错误!未找到引用源。**. Curve #1 in the figure shows the average tensile strengths at different temperatures, which were measured by UTST. It can be seen that the average tensile strength increases with the temperature rising from relatively low value to a maximum and then drops quickly. Curve #3 illustrates the development of the cooling-related tensile stress from the cooling test. With the decrease of the test temperature, the cooling-related tensile stress gradually increases until it reaches σ_F at the temperature T_F. At this point, the average tensile strength curve and cooling-related tensile stress curve intersect, and the sample breaks due to the tensile stress induced by the temperature drop. The difference between Curves #1 and #3 is Curve #2, which is defined as tensile strength reserve (TSR). It indicates the maximum permissible tensile strength of the pavement surface course to bear traffic loads. Obviously, when the temperature is T_F, the tensile strength reserve is zero, which means the road material has no residual tensile strength to bear traffic loads. With the increase of the temperature from T_F, the tensile strength reserve increases until a maximum $\Delta\beta_{t,max}$, which is at the temperature of $T(\Delta\beta_{t, max})$ and then decreases gradually.

2.3 Functional Performance: Acoustic Properties

Tire-road noise is the consequence of the superposition of several uncorrelated sound sources (Beckenbauer et al., 2002, Möser, 2012, Altreuther and Bartolomaeus, 2008, Schacht, 2015). Each sound source is related to a particular sound generation mechanism. In this study, the acoustic performance of the PERS and PA samples were characterized by measuring their acoustic absorption, which is the major factor affecting the tire-road noise of porous pavement.

The acoustic absorption was measured by the impedance tube test in accordance with EN ISO 10534-2: “Acoustics determination of sound absorption coefficient and impedance in impedance tubes - Part 2: Transfer-function method (ISO 10534-2:1998)”. As **错误!未找到引用源。** illustrates, the impedance tube is a straight rigid smooth and air-tight tube, fitted with a speaker on one end and the sample at the other end. The sample holder is a separate unit which is attached to the tube for measurement. The diameter of the samples, which is the same as the inside diameter of the impedance tube, was 50 mm in this study. The sample holder can be adjusted to the height of the sample by means of a piston and was set to be level with the bottom side of the sample to prevent any cavities, thus creating an acoustically hard end point. The impendence tube has an acoustically hard inner lining, forcing the sound to propagate along the longitudinal direction. If the diameter of the tube is smaller than the wave length, the sound waves propagate only in longitudinal direction (Schacht, 2015, Altreuther and Bartolomaeus, 2008, Möser, 2012, Beckenbauer et al., 2002).

The speaker sweeps through a given frequency range, creating plane waves in the tube. The sound pressure is measured at two points in close proximity to the sample by the microphones attached to the tube wall. The complex acoustical transfer functions of the two microphone signals are determined and used to calculate the complex reflection factor, absorption factor and the acoustic impedance of the sample material in accordance with EN ISO 10534-2. The absorption factor is given as a function of the frequency. The applicable frequency ranges may be adjusted by varying the diameter of the tube and/or varying the distance between the microphones.

2.4 Functional Performance: De-icing Capability

In order to quantify the difference in deformation of the ice layers at the surfaces of PERS and PA under external forces, the impact tests were carried out on both types of samples.

The thickness of the ice layers formed on top of PERS and PA was 5 mm. The hammer with a weight of 4.5 kg and diameter of 75 mm freely dropped from a height of 45 cm onto the ice layer, as shown in 错误!未找到引用源。. Then, pictures were taken after each impact conducted by the hammer to compare the different deformation of the ice layer.

2.5 Numerical Simulation

In order to investigate the mechanical responses of the pavements surfaced with PERS or PA, numerical simulation by using self-developed finite element (FE) software SAFEM (Liu et al., 2016b, Liu et al., 2016a) was carried out. The SAFEM is a three-dimensional (3D) FE program that requires only a two-dimensional (2D) mesh by incorporating the semi-analytical method using Fourier series in the third dimension. The parallel computing technology can be applied easily in this code. As a result, the computation time could be significantly reduced. The typical 3D SAFEM model for the pavement problem is shown in 错误!未找到引用源。.

The responses from the SAFEM model were evaluated using the pavement structure as shown in 错误!未找到引用源。, which is widely used in the cold regions in Germany.

The load was assumed to be the load from a typical truck with tandem axles and single tires, the axle load of which was 7000 kg. The distances between the two axles and tires from one axle were 6600 mm and 2500 mm, respectively. According to (FGSV, 2009), the shape of the contact area was assumed to be a circle with a radius of 15 cm. Therefore, the uniformly distributed contact pressure was 0.485 MPa. The thickness of the sub-grade was 200 cm. Such a large value was selected to minimize the influence of the boundary condition on the results. The excess lengths in the traffic direction and the transverse direction were 20 times of the loading radius to limit the time required for the mesh generation and the following computational calculation. These definitions were found to be able to best balance the accuracy and efficiency in the simulation based on a large number of investigations. The bottom nodes of the mesh representing sub-grade in the SAFEM were fixed in all directions. Pavements with no ice layer or ice layers of 5 mm and 10 mm were simulated at two different temperatures of -25°C and -10°C. The ice layer, surface layer (PERS or PA) and asphalt base layer were completely bonded at the interfaces; the two interfaces among the asphalt base course, frost protection layer and sub-grade were partially bonded, which means the nodes at the interfaces between the different layers always have the same displacements in the vertical direction but may have different displacements in the horizontal direction. The material property parameters are listed in 错误!未找到引用源。.

3. RESULTS AND ANALYSIS

3.1 Mechanical Performance

Resistance against low temperature cracking

The tensile strength reserves of PERS and PA were calculated based on the results of UTST and cooling tests, which are shown in 错误!未找到引用源。. The development trends of the average tensile strength, cooling-related tensile stress and tensile strength reserve of the PA samples are consistent with the representative example shown in 错误!未找到引用源。, while those of the PERS samples show entirely different variation at different temperatures. The average tensile strength of the PERS gradually increases with the decrease of temperature, and the growth rate becomes even higher. The cooling-related tensile stress remains extremely low which is near zero when the temperature is above 10°C, and even when the temperature reaches -33°C, this value is still very small (0.05 N/mm^2). As a result, the tensile strength reserve of the PERS is close to the average tensile strength, which means the tensile stress induced by the temperature can almost be ignored and theoretically the average tensile strength of the road can be used to bear the traffic loads.

As 错误!未找到引用源。 (a) shows, the tensile strength reserve of the PERS is higher than that of the PA at the temperature between -33°C and -23°C, which proves the PERS has better bearing capacity of traffic loads in cold regions at extremely low temperature. When the temperature increases from 23°C to 11°C, the tensile strength reserve of the PERS is lower than that of the PA, but its decay rate becomes smaller, and when the temperature is above 11°C, the tensile strength reserve of the PERS is higher again. From 错误!未找到引用源。 (b), it can be seen that the ultimate tensile strain of the PERS is much larger than that of the PA in the whole test temperature range, which implies a longer cracking stage or duration needed by PERS sample at break.

3.2 Functional Performance

3.2.1 Acoustic properties

错误!未找到引用源。 shows the absorption coefficients of the PERS samples in comparison to PA. It can be seen that the absorption coefficients of the PERS samples are within the range of 60% to 95% between 800 Hz and 2500 Hz, which is the crucial frequency range to human auditory perception. From 200 Hz to 6000 Hz, PERS shows two maximum absorption coefficients: 95% and 82%, at 1500 Hz and 4000 Hz, respectively. The general courses of the absorption coefficients correspond well with the measurements reported by the study conducted in Stockholm (Sandberg et al., 2005, Sandberg and Kalman, 2005). The maximum absorption coefficients of PERS are similar to those of PA but much wider. It is worth noting that the precise frequency corresponding to the maximum absorption coefficient is a function of the layer thickness, and is not material dependent. In addition to the absolute values of the maximum absorption coefficient, it is important to compare the course of the absorption coefficient over the frequency. It can be seen that the PERS samples exhibit wider maximum peaks compared with the PA, which is an indicator of better noise absorption.

3.2.2 Deformation of ice layer

The deformations of the ice layer on top of PA and PERS under the impact conducted by dropping hammer are shown in 错误!未找到引用源。 and 错误!未找到引用源。, respectively. Compared with the deformation after four-time impacts, the deformation of ice layer after one-time impact is obviously smaller in both samples. Moreover, the deformation of ice layer on the PERS surface is clearly larger than that on the PA surface after both one-time impact and four-time impacts. It indicates that the ice layer formed on the PERS surface is much easier to be destroyed under the same external force than that on the PA, which is more suitable to be applied in cold regions.

3.3 Numerical Simulation

3.3.1 Mechanical performance of pavement surface materials

The mechanical responses of pavements under traffic loads, such as displacements, strains and stresses, are able to be fast and accurately computed by SAFEM. For example, **错误!未找到引用源。** shows the computational stresses for the pavement model with PERS materials and an ice layer of 10mm in thickness at -25°C. In order to facilitate the observation of the distribution of the stress, sectional views are also provided in addition to the full views of the pavement model.

错误!未找到引用源。 and **错误!未找到引用源。** illustrate the horizontal stresses along the transverse direction of traffic loads derived from different pavement surface materials at -10°C and -25°C, respectively. The development trend of the horizontal stress from the same pavement surface material is similar at different temperatures. Therefore, only the development curves of the stress at the top of pavement surfaces without ice layer are provided in **错误!未找到引用源。**(a) and **错误!未找到引用源。**(a). The offset is from the midpoint of the first axle to the right curbside of the pavement. The maximum compressive stresses from both pavements obviously decrease when the ice layer forms and increases in thickness at the pavement surface, which can be seen from **错误!未找到引用源。**(b) and **错误!未找到引用源。**(b). Temperature has little effect on the stress of the pavements with PA surface or PERS surface when no ice layer forms at the pavement surface. If the ice layer exists, the maximum compressive stresses decrease with dropping temperature and significant change occurs in the stress from PA surface. It is worth noting that the maximum compressive stress of the pavement with PERS surface is much less than that of PA at the same temperature and with the same ice thickness, and the pavement with PA surface exhibits a large tensile stress at the offsets of 0 and 2800 mm, whereas PERS does not, which means the pavement with PA surface is more prone to surface cracks.

3.3.2 Capability of de-icing

The maximum vertical displacement at the ice layer surface is shown in 错误!未找到引用源。. The deformation of the ice layer shows a decreasing trend with the increase of the ice layer thickness or the decrease of the temperature. Moreover, the deformation of the ice layer on the pavement with PERS surface is larger than the corresponding case with PA surface, which indicates that the pavement with PERS surface has more capability of de-icing than PA.

The maximum horizontal strains along the transverse direction of traffic derived from the two pavement surfaces are shown in 错误!未找到引用源。. As can be seen from the figures, the strain of PERS is significantly greater than that of PA. Because the deformation of PERS is larger than PA, the interface bonding between PERS and the ice layer breaks more easily, so that the ice layer on PERS surface is more prone to be stripped off and broken. Meanwhile, with the decrease of temperature, the strains of PA decrease more significantly than those of PERS, which indicates that the deformation of PA is reduced more and thus its capability of de-icing is decreased more. As a result, PERS is more suitable for the urban roads in cold regions than PA.

4. FINDINGS AND RECCOMMENDATIONS

This study investigated the suitability of PERS for urban roads in cold regions regarding mechanical and functional performances by means of experiments and numerical simulation. The following summarizes the major findings of this study:

- The tensile strength reserve of the selected PERS is close to the average tensile strength and higher than that of the PA within the temperature range of -33°C and -23°C, which proves the PERS has better bearing capacity of traffic loads in cold regions at extremely low temperature.
- The ultimate tensile strain of the PERS is much larger than that of the PA, which means a longer cracking stage or duration needed for PERS samples to break.
- The maximum absorption coefficients of the PERS are significantly higher and the PERS samples exhibit wider maximum peaks compared with the PA, indicating the PERS has better noise absorption capability.
- The impact test revealed that the ice layer formed on top of the PERS is much easier to be destroyed under the same external force than that on top of the PA.
- The pavement with PA surface exhibits a large tensile stress at some specific offset locations from the loads, whereas PERS does not, implying the pavement with PA surface is more prone to surface cracks.
- The deformation of the ice layer on the pavement with PERS surface is larger than that with PA surface at the same temperature, which indicates that the pavement with PERS surface has better capability to de-ice than PA.
- The maximum horizontal strain of the pavement with PERS surface is larger than that with PA, and the interface bonding between PERS and the ice layer breaks more easily. Thus, the ice layer on PERS surface is more prone to be stripped off and broken.

Based on the above findings, the suitability of PERS for urban streets in cold region is basically proved. But the field performance of PERS in urban roads in cold regions should be investigated in the further research. In addition, microscopic analysis is recommended to be further conducted so that the influence of different components of PERS can be quantified and the performance of the PERS such as the tensile strength can be optimized by changing the mixing design.

ACKNOWLEDGMENTS

The authors acknowledge the sponsorship of the German Research Foundation (DFG) on the work presented in this paper through Research Grant OE 514/4-1.

REFERENCES

Altreuther, B. & Bartolomaeus, W. 2008. Acoustical Characterisation And Life-Cycle Of Porous Road Surfaces. *Journal Of The Acoustical Society Of America,* 123**,** 3391.

Amundsen, A., Klaeboe, R 2005. A Nordic Perspective On Noise Reduction At The Source. Institute Of Transport Economics.

Arand 1991. Verhalten Von Nähten In Asphaltdeckschichten Bei Kälte [Behaviour Of Joints In Asphalt Surface Layer Under Cold Conditions]. *Die Asphaltstraße [The Asphalt Road],* 6**,** 17-25.

Beckenbauer, T., Spiegler, P. & Vanblokland, G. 2002. *Einfluss Der Fahrbahntextur Auf Das Reifen-Fahrbahn-Geräusch*.

Biligiri, K. P., Kalman, B. & Samuelsson, A. 2013. Understanding The Fundamental Material Properties Of Low-Noise Poroelastic Road Surfaces. *International Journal Of Pavement Engineering,* 14**,** 12-23.

De Almeida J Nior, A. F., Battistelle, R. A., Bezerra, B. S. & De Castro, R. 2012. Use Of Scrap Tire Rubber In Place Of Sbs In Modified Asphalt As An Environmentally Correct Alternative For Brazil. *Journal Of Cleaner Production,* 33**,** 236-238.

Estevez, M. 2009. Use Of Coupling Agents To Stabilize Asphalt–Rubber–Gravel Composite To Improve Its Mechanical Properties. *Journal Of Cleaner Production,* 17**,** 1359-1362.

FEHRL 2006. Guidance Manual Or The Implementation Of Low-Noise-Road Surfaces.

FGSV 2009. *Guidelines For The Computational Dimension Of The Upper Structure Of Road With Asphalt Surface Course,* Cologne, Research Society For Road And Transportation, 2009 Edition.

Goubert, L. Developing A Durable And Ultra Low Noise Poroelastic Pavement. Proc. Of Inter-Noise, 2014.

Goubert, L., Bendtsen, H., Bergiers, A., Kalman, B. & Kokot, D. 2016. The Poroelastic Road Surface (Pers): Is The 10 Db Reducing Pavement Within Reach? *Materials And Infrastructures 1***,** 253-268.

Kalman, B., Biligiri, K. P. & Sandberg, U. Project Persuade: Optimization Of Poroelastic Road Surfaces In The Laboratory. 40th International Congress And Exposition On Noise Control Engineering 2011 (Inter-Noise 2011). Proceedings Of A Meeting Held 4-7 September 2011, Osaka, Japan, 2011. Institute Of Noise Control Engineering Of Japan (Ince/J), Acoustical Society Of Japan (Asj), 699-707.

Leng, Z., Yu, H., Zhang, Z. & Tan, Z. 2017. Optimizing The Mixing Procedure Of Warm Asphalt Rubber With Wax-Based Additives Through Mechanism Investigation And Performance Characterization. *Construction And Building Materials,* 144**,** 291-299.

Liu, P., Wang, D., Hu, J. & Oeser, M. 2016a. Safem–Software With Graphical User Interface For Fast And Accurate Finite Element Analysis Of Asphalt Pavements. *Journal Of Testing And Evaluation,* 45.

Liu, P., Wang, D., Otto, F., Hu, J. & Oeser, M. 2016b. Application Of Semi-Analytical Finite Element Method To Evaluate Asphalt Pavement Bearing Capacity. *International Journal Of Pavement Engineering***,** 1-10.

Moser, M. 2012. *Technische Akustik*, Springer-Verlag.

Meiarashi. Porous Elastic Road Surface As An Ultimate Highway Noise Measure. The Xxiind Piarc World Road Congress, 2003.

Moon, K. H., Falchetto, A. C. & Marasteanu, M. O. 2014. Investigation Of Limiting Criteria For Low Temperature Cracking Of Asphalt Mixture. *Ksce Journal Of Civil Engineering,* 18**,** 172-181.

Pigasse, G., Jensen, M. & Bendtsen, H. 2012. Cost-Benefit Analysis Of A Poroelastic Road Surface. *Euronoise Prague***,** 10-13.

Presti, D. L. 2013. Recycled Tyre Rubber Modified Bitumens For Road Asphalt Mixtures: A Literature Review. *Construction And Building Materials,* 49**,** 863-881.

Sandberg, U. & Goubert, L. Persuade: A European Project For Exceptional Noise Reduction By Means Of Poroelastic Road Surfaces. 40th International Congress And Exposition On Noise Control Engineering 2011 (Inter-Noise 2011), 2011. Institute Of Noise Control Engineering Of Japan (Ince/J), Acoustical Society Of Japan (Asj), 673-684.

Sandberg, U., Goubert, L., Biligiri, K. P. & Kalman, B. 2010. State-Of-The-Art Regarding Poroelastic Road Surfaces. *Deliverable D8,* 1.

Sandberg, U. & Gucbert, L. Pooelastic Road Surface (Pers): A Review Of 30 Years Of R And D Work. Inter-Noise And Noise-Con Congress And Conference Proceedings, 2011. Institute Of Noise Control Engineering, 3014-3021.

Sandberg, U. & Kalman, B. The Poroelastic Road Surface–Results Of An Experiment In Stockholm. Proceedings Of Forum Acusticum, 2005. 834-0.

Sandberg, U., Kalman, B. & Nilsson, R. 2005. Design Guidelines For Construction And Maintenance Of Poroelastic Road Surfaces. *Silvia Project Report Silvia-Vti-005-02-Wp4-141005*.

Schacht, A. 2015. Entwicklung Kuenstlicher Strassendeckschichtsysteme Auf Kunststoffbasis Zur Geraeuschreduzierung Mit Numerischen Und Empirischen Verfahren. *Aachener Mitteilungen Strassenwesen, Erd-Und Tunnelbau*.

Schacht, A., Wang, D. & Steinauer, B. 2011. Untersuchung Der Kornausbrueche Bei Poro-Elastischen Fahrbahnbelaegen Mit Dem Aachener-Ravelling-Tester (Arte)/Investigation Of The Granule Loss Of Poroelastic Road Surfaces Using The Aachener-Ravelling-Tester (Arte). *Bauingenieur,* 86.

Shu, X. & Huang, B. 2014. Recycling Of Waste Tire Rubber In Asphalt And Portland Cement Concrete: An Overview. *Construction And Building Materials,* 67**,** 217-224.

Siddique, R. & Naik, T. R. 2004. Properties Of Concrete Containing Scrap-Tire Rubber–An Overview. *Waste Management,* 24**,** 563-569.

Singh, S., Nimmo, W., Gibbs, B. & Williams, P. 2009. Waste Tyre Rubber As A Secondary Fuel For Power Plants. *Fuel,* 88**,** 2473-2480.

Teltayev, B. 2014. Evaluation Of Low Temperature Cracking Indicators Of Hot Mix Asphalt Pavement. *International Journal Of Pavement Research And Technology,* 7**,** 343-351.

Wang, D., Chen, X., Stanjek, H., Oeser, M. & Steinauer, B. 2014. Influence Of Freeze–Thaw On The Polishing Resistance Of Coarse Aggregates On Road Surface. *Construction And Building Materials,* 64**,** 192-200.

Wang, D., Chen, X., Xie, X., Stanjek, H., Oeser, M. & Steinauer, B. 2015. A Study Of The Laboratory Polishing Behavior Of Granite As Road Surfacing Aggregate. *Construction And Building Materials,* 89**,** 25-35.

Wang, D., Chen, X., Yin, C., Oeser, M. & Steinauer, B. 2013. Influence Of Different Polishing Conditions On The Skid Resistance Development Of Asphalt Surface. *Wear,* 308**,** 71-78.

Wang, D., Schacht, A., Leng, Z., Leng, C., Kollmann, J. & Oeser, M. 2017. Effects Of Material Composition On Mechanical And Acoustic Performance Of Poroelastic Road Surface (Pers). *Construction And Building Materials,* 135**,** 352-360.

Wen, Z., Zhang, M., Ma, W., Wu, Q., Niu, F., Yu, Q., Fan, Z. & Sun, Z. 2015. Thermal–Moisture Dynamics Of Embankments With Asphalt Pavement In Permafrost Regions Of Central Tibetan Plateau. *European Journal Of Environmental And Civil Engineering,* 19**,** 387-399.

Yu, H., Leng, Z., Xiao, F. & Gao, Z. 2016. Rheological And Chemical Characteristics Of Rubberized Binders With Non-Foaming Warm Mix Additives. *Construction And Building Materials,* 111, 671-678.

Yu, H., Leng, Z., Zhou, Z., Shih, K., Xiao, F. & Gao, Z. 2017. Optimization Of Preparation Procedure Of Liquid Warm Mix Additive Modified Asphalt Rubber. *Journal Of Cleaner Production,* 141, 336-345.

LIST OF FIGURES AND TABLES

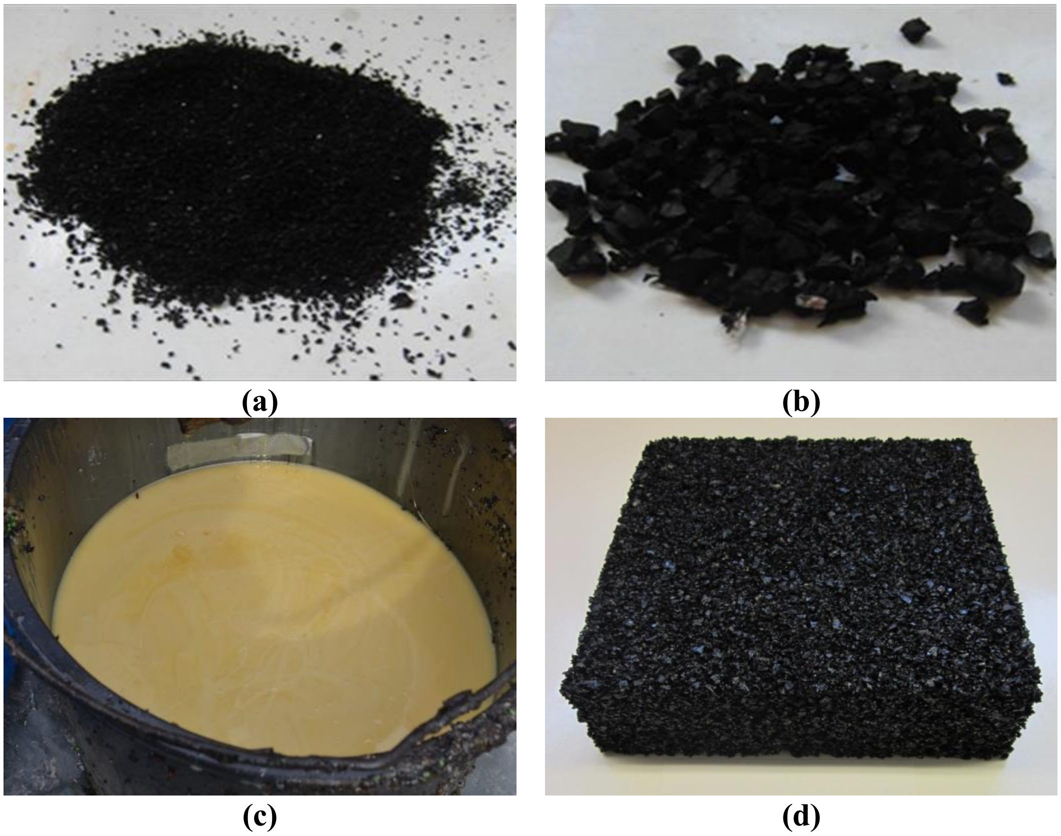

FIGURE 19 Components and Test Sample of PERS: (a) Fine rubber granules; (b) Coarse rubber granules, (c) Polyurethane binder; (d) PERS sample

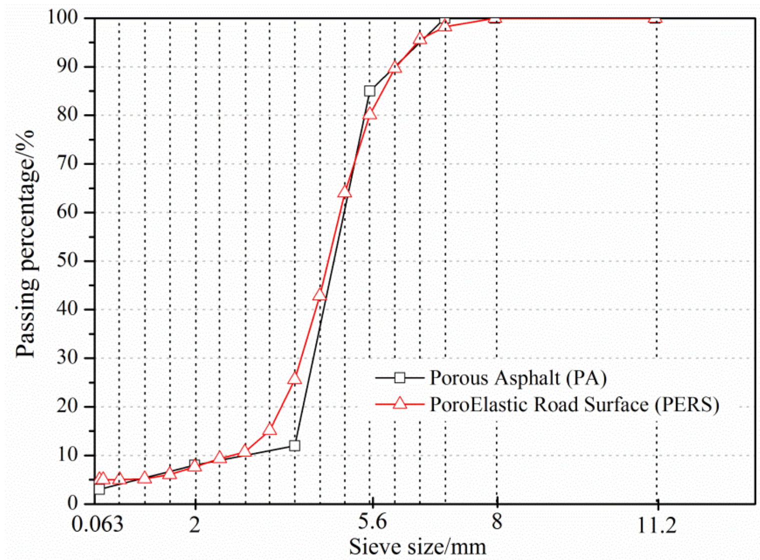

FIGURE 20 Graphical Representation of the Determination of Tensile Strength Reserve

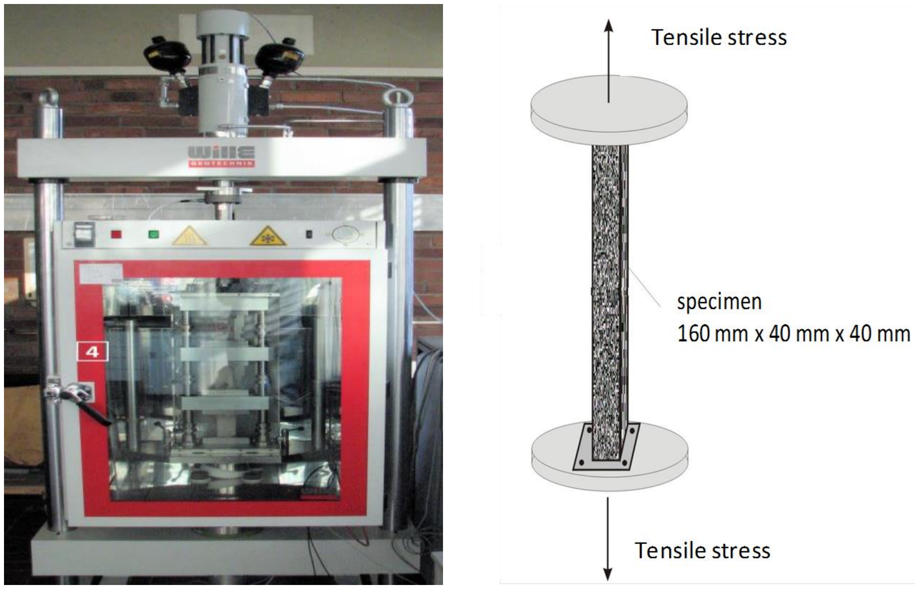

(a) **(b)**

FIGURE 21 Uniaxial Tension Stress Test (UTST): (a) Testing Machine; (b) Testing Specimen

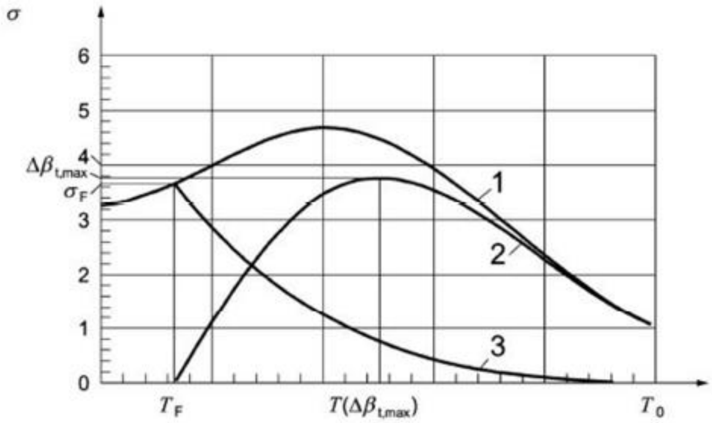

FIGURE 22 Determination of Tensile Strength Reserve according to EN 12697-46 and (Arand, 1991)

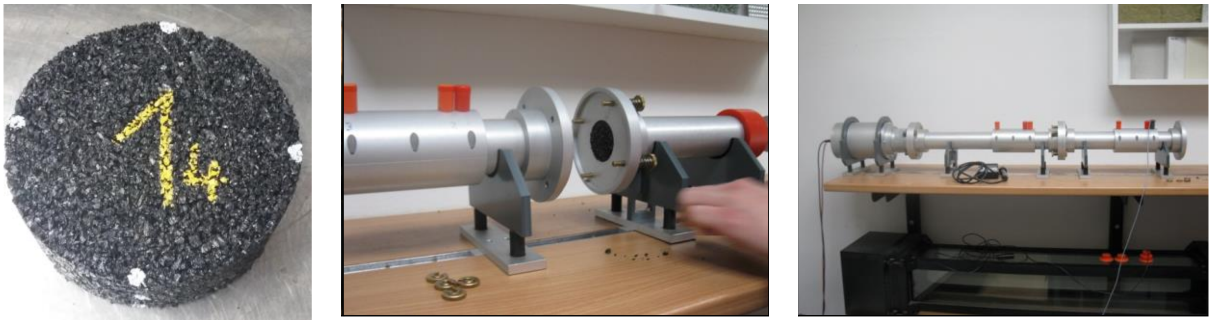

(a) (b) (c)

FIGURE 23 Setup of the impedance tube for measuring absorption properties of material samples: (a) PERS sample; (b) attaching sample holder to the tube; (c) outside appearance of the whole device (Beckenbauer et al., 2002)

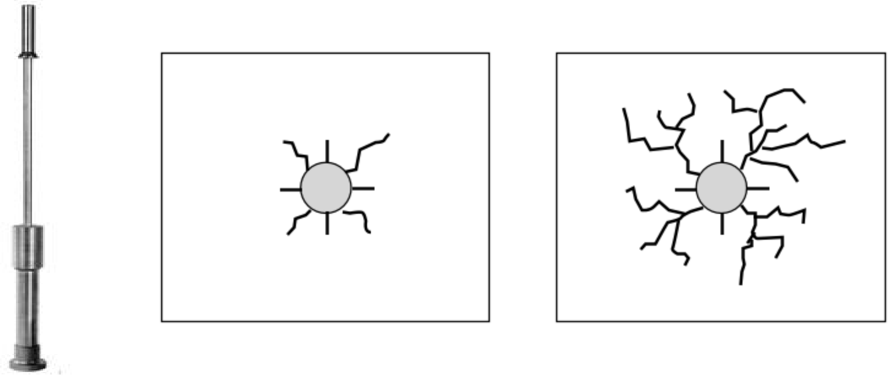

(a) **(b)**

FIGURE 24 Impact Test: (a) Setup of the device; (b) Representation of ice layer deformation after impact

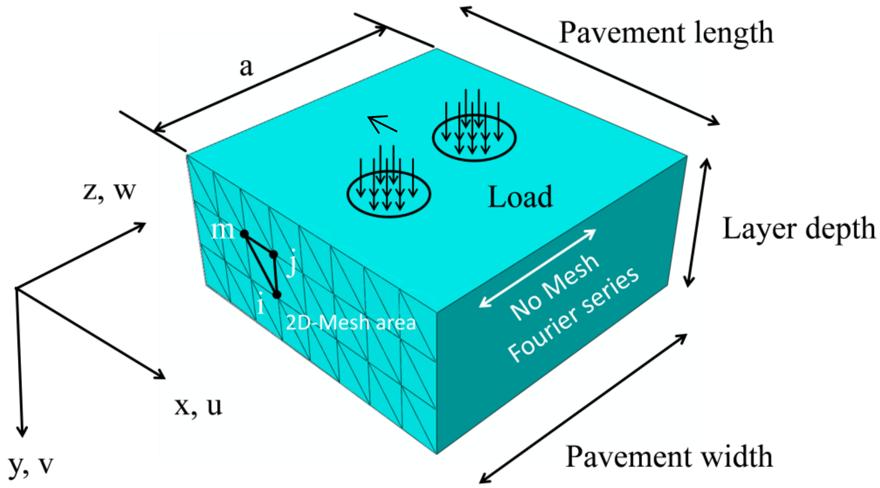

FIGURE 25 A Typical SAFEM model

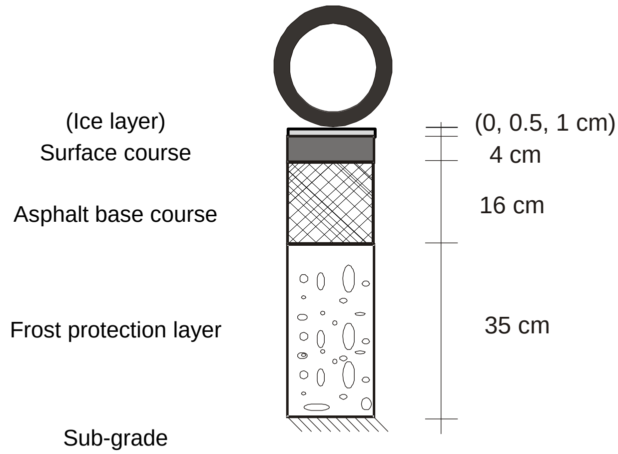

FIGURE 26 Pavement Structure for Numerical Analysis

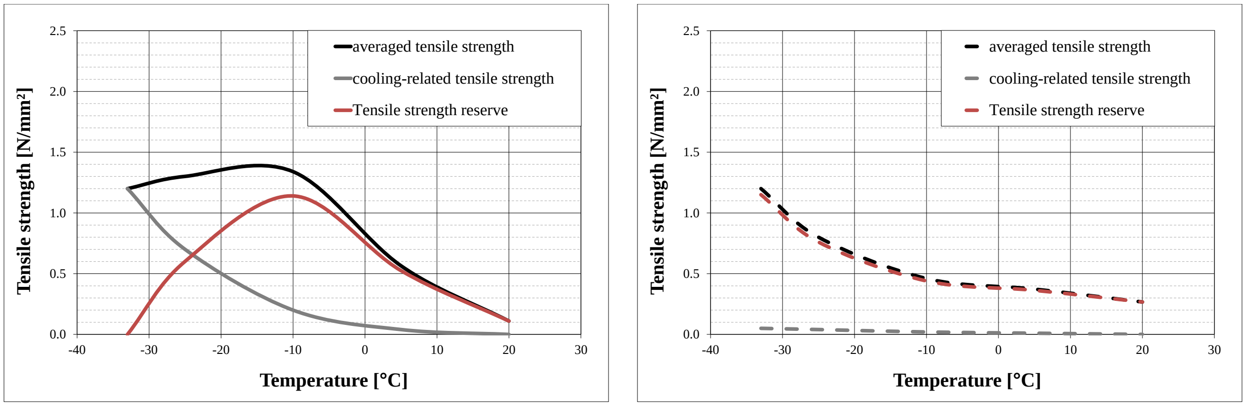

(a) **(b)**

FIGURE 27 Determination of Tensile Strength Reserve: (a) PA; (b) PERS.

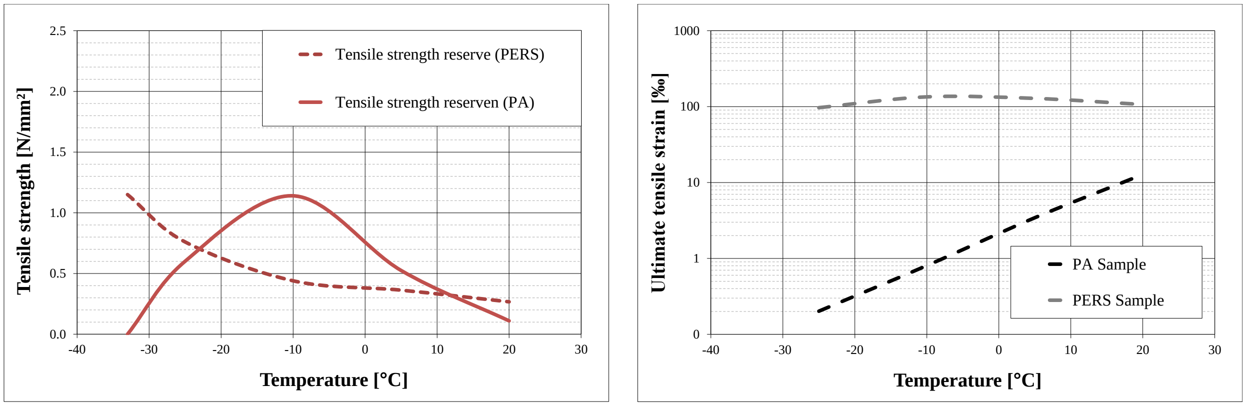

(a) **(b)**

FIGURE 28 Comparison of PERS and PA: (a) Tensile Strength Reserve; (b) Ultimate Tensile Strain

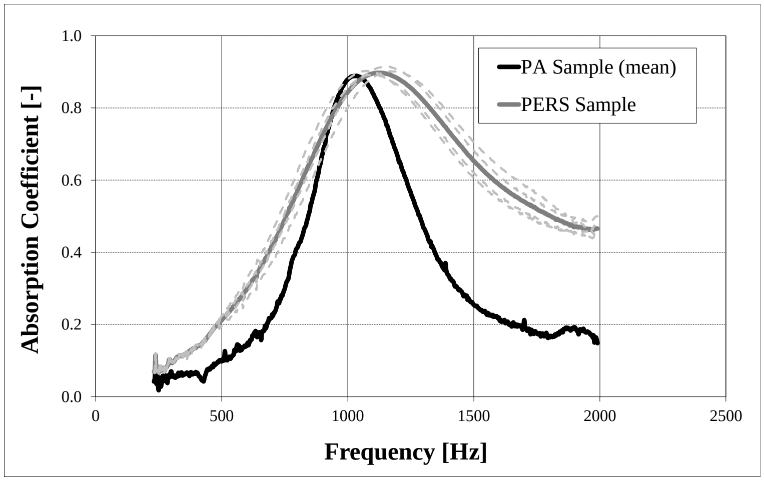

FIGURE 29 Absorption coefficient curves measurements in accordance with ISO 10534-2

(a) (b)

FIGURE 30 Deformation of ice layer on PA surface under impact of drop hammer: (a) One-time impact; (b) Four-time impacts

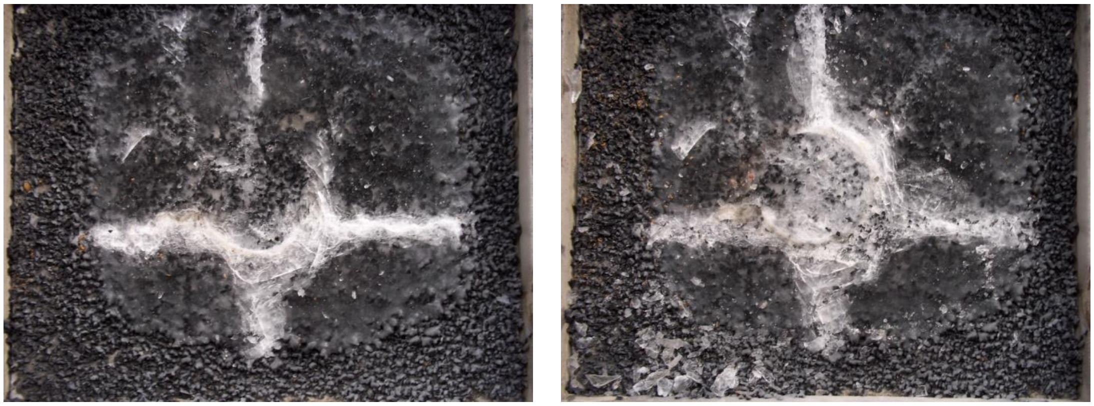

(a) **(b)**

FIGURE 31 Deformation of ice layer on PERS surface under impact of drop hammer: (a) One-time impact; (b) Four-time impacts

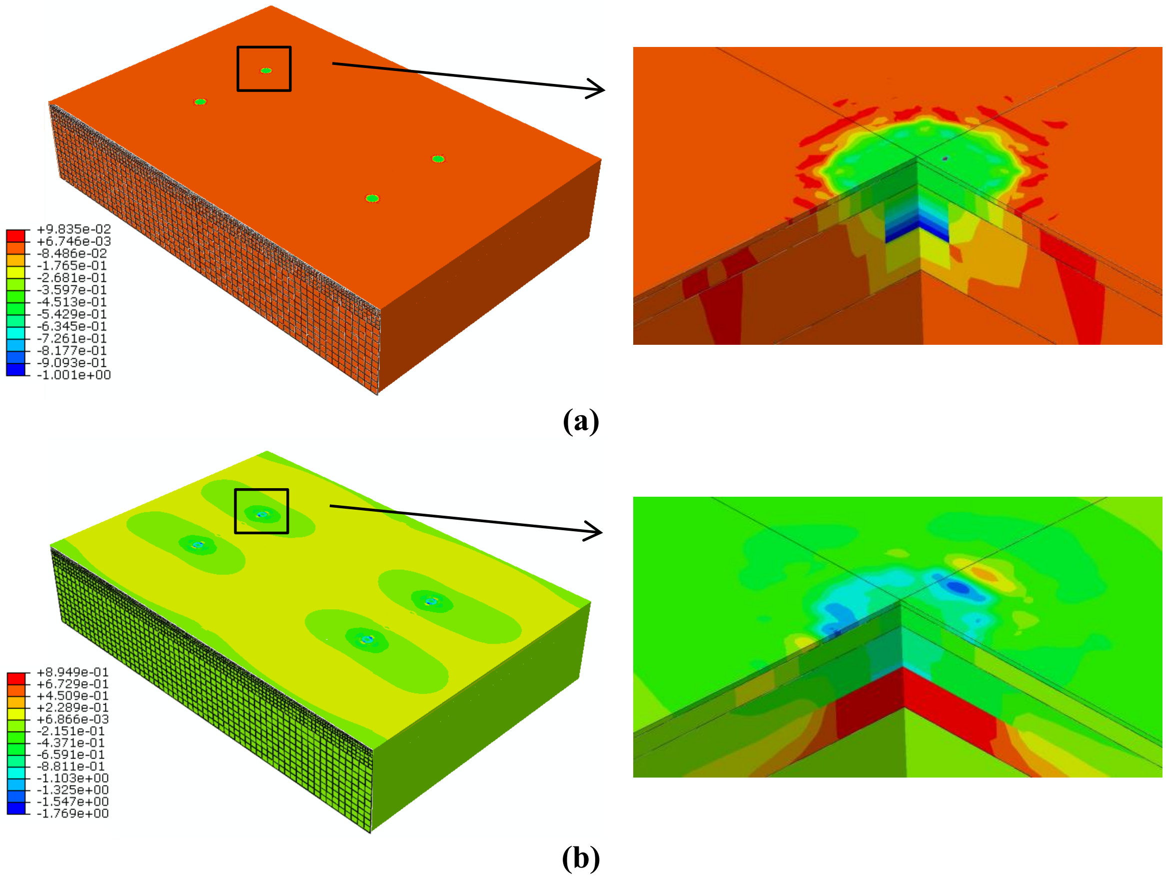

FIGURE 32 The computational stresses and deformation: (a) vertical stress; (b) horizontal stress along transverse direction

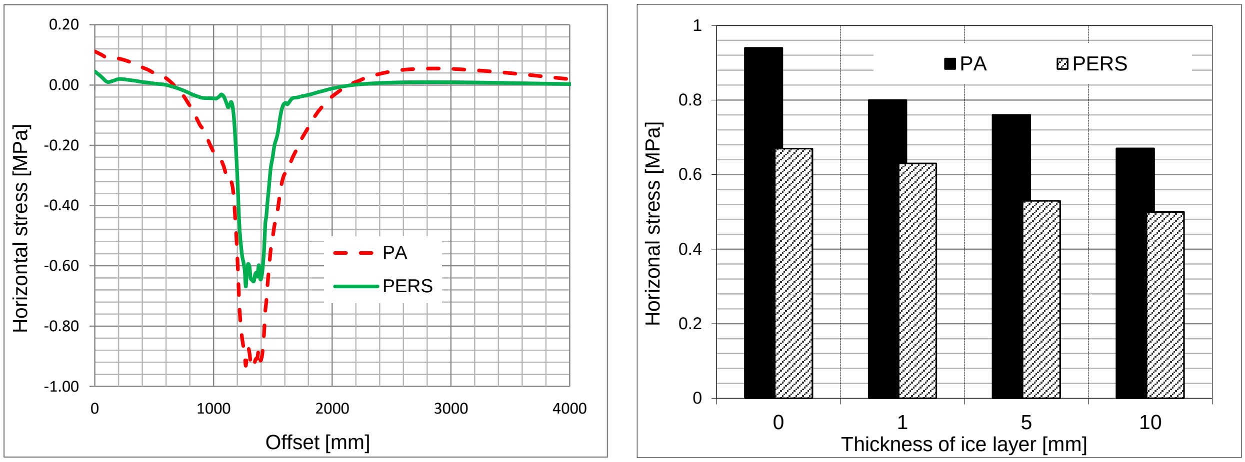

(a) **(b)**

FIGURE 33 Horizontal stress along transverse direction at -10 °C: (a) development of the stress at the top of pavement surface without ice layer; (b) maximum stresses from different thicknesses of ice layer

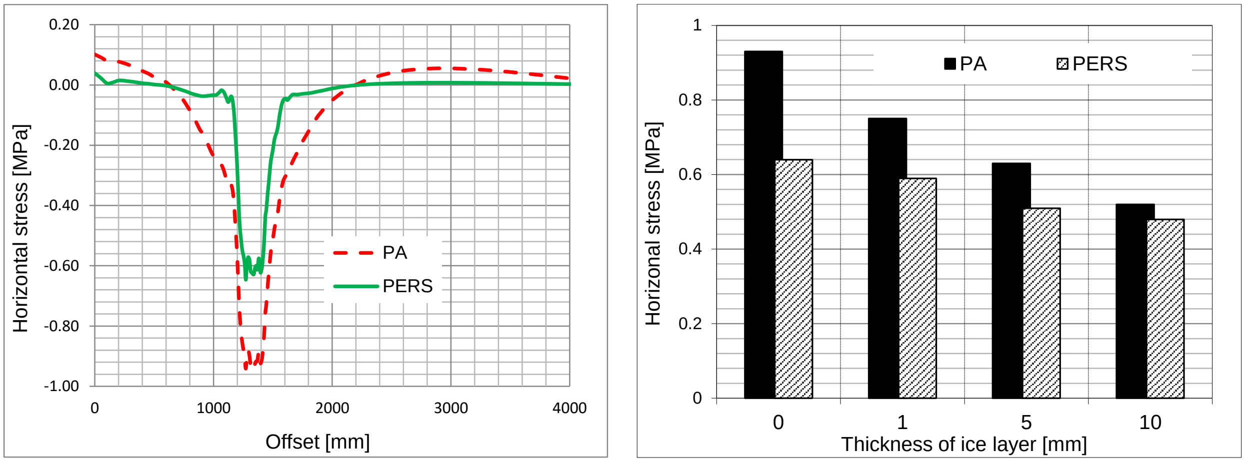

(a) **(b)**

FIGURE 34 Horizontal stress along transverse direction at -25 °C: (a) development of the stress at the top of pavement surface without ice layer; (b) maximum stresses from different thicknesses of ice layer

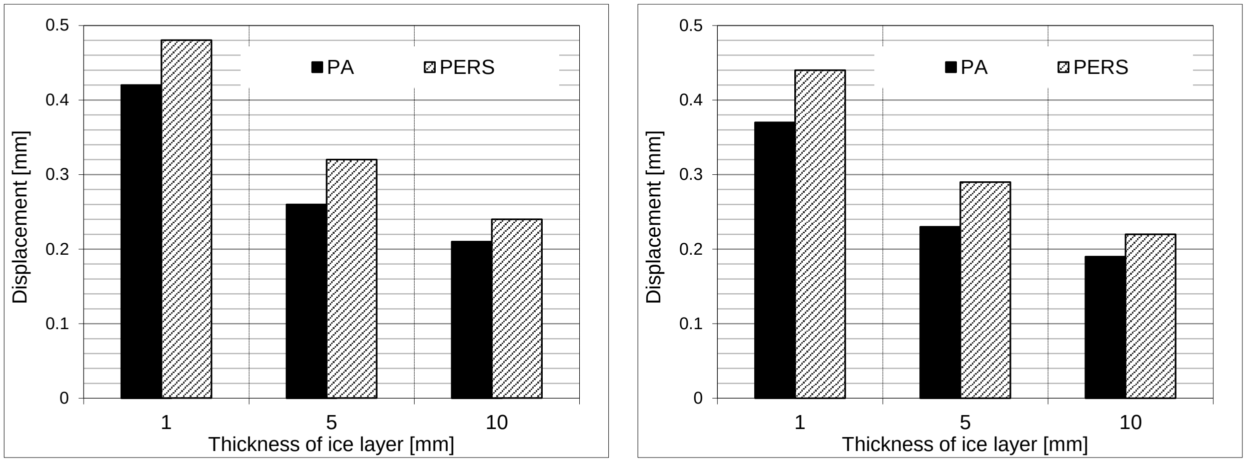

(a) **(b)**

FIGURE 35 Deformation of the ice layer: (a) at -10 °C; (b) at -25 °C

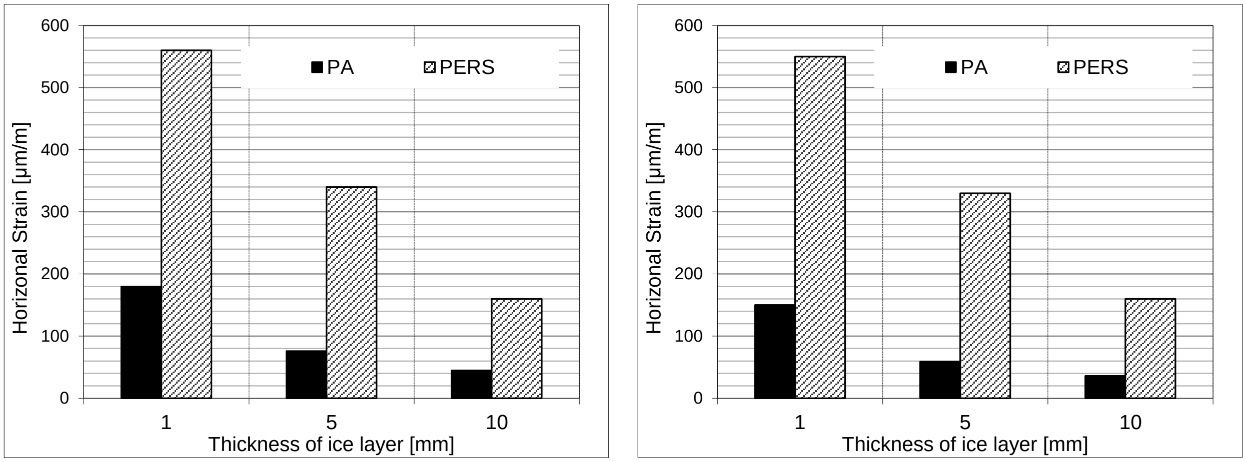

(a) **(b)**

FIGURE 36 Maximum horizontal strain at the top of surface course: (a) at -10 °C; (b) at -25 °C

Table 2 Material properties of the pavement.

Layer	-25 °C				-10 °C			
	PA		PERS		PA		PERS	
	E [MPa]	μ	E [MPa]	μ	E [MPa]	μ	E [MPa]	μ
Ice layer	9670	0.36	9670	0.36	9480	0.36	9480	0.36
Surface course	11674.7	0.35	1000	0.47	8750	0.35	1000	0.47
Asphalt base course	26720	0.35	26720	0.35	18796.8	0.35	18796.8	0.35
Frost protection layer	120	0.49	120	0.49	120	0.49	120	0.49
Sub-grade	45	0.49	45	0.49	45	0.49	45	0.49